# Deletion, Methylation, and Expression of the *NKX3.1* Suppressor Gene in Primary Human Prostate Cancer

**Ekatherine Asatiani, Wen-Xin Huang, Antai Wang, Elizabeth Rodriguez Ortner, Luciane R. Cavalli, Bassem R. Haddad, and Edward P. Gelmann**

Departments of Oncology and Medicine, Lombardi Comprehensive Cancer Center, Georgetown University, Washington, District of Columbia

## Abstract

**NKX3.1 is a prostate-specific homeoprotein and tumor suppressor that is affected by the loss of 8p21 in prostate cancer. In mice, *Nkx3.1* haploinsufficiency results in prostatic dysplasia and complements cancer formation induced by loss of other suppressor genes. However, NKX3.1 expression can be immunohistochemically detected in most primary prostate cancers. We examined the relationship between suppressor gene haploinsufficiency, methylation, and quantitative NKX3.1 expression levels in primary prostate cancer. *NKX3.1* gene copy number was assessed by microsatellite analysis, fluorescence *in situ* hybridization, and quantitative PCR. *NKX3.1* gene methylation was determined in prostate cancer cell lines and we thereby identified potential CpG methylation sites for methylation-specific PCR analysis in tissues. We validated and then applied an internally controlled fluorescence immunomicroscopic assay for NKX3.1 protein expression in 48 primary prostate cancer specimens from radical prostatectomies. *NKX3.1* loss of heterozygosity was found in 27 of 43 tissues tested. Classic CpG island methylation of the *NKX3.1* gene was not found in either prostate cancer cell lines or tissues. However, in 33 of 40 samples tested, CpG sites at −921, −903, and −47 were methylated to a greater degree in malignant than in adjacent normal cells. In 43 of 48 samples, NKX3.1 protein expression was reduced from 0.34 to 0.90 compared with adjacent normal luminal epithelium (mean of all samples, 0.68; 95% confidence interval, 0.05). In 12 cases that also had high-grade prostatic intraepithelial neoplasia, NKX3.1 expression levels were similar in preinvasive and invasive cancer cells and significantly lower than adjacent normal cells. Even in the presence of allelic loss, NKX3.1 expression is reduced over a wide range in prostate cancer at the time of prostatectomy, suggesting that diverse factors influence expression. Samples with protein expression below the median level in cancer cells had both *NKX3.1* deletion and selective CpG methylation.** (Cancer Res 2005; 65(4): 1164-73)

## Introduction

Adenocarcinoma of the prostate, like many epithelial malignancies, initiates in epithelial cells in the prostate that acquire the precursor or gatekeeper mutations required for the malignant phenotype. As with other carcinomas, the search for the initiating mutations in prostate cancer has been guided by identification of chromosomal loci that frequently undergo loss of heterozygosity (LOH). LOH in sporadic prostate cancer most commonly occurs at chromosomal locus 8p21.2 (1–3). The minimally deleted region of 8p21.2 that may be lost in up to 85% of prostate cancer cases contains the gene for the prostate-specific homeodomain protein NKX3.1 (4). NKX3.1 is expressed specifically in prostate luminal epithelial cells and undergoes progressive loss of protein expression with prostate cancer progression to hormone-independence and metastases (5). The *NKX3.1* gene is not subject to somatic mutation in prostate cancer (6, 7), but gene-targeting studies in mice showed that *Nkx3.1* haploinsufficiency can predispose to prostate epithelial dysplasia and can cooperate with other oncogenic mutations to augment carcinogenesis (8, 9). In gene-targeted mice, *Nkx3.1* haploinsufficiency is accompanied by decreased expression of genes under the regulation of the Nkx3.1 homeoprotein (10). The data are highly suggestive that NKX3.1 is both suppressor protein and is inactivated at the earliest stages of human prostate cancer.

In general, tumor suppressor genes undergo biallelic disruption that results in complete loss of suppressor function to contribute to carcinogenesis. In some cases, reduced levels of a suppressor protein are sufficient to affect cell phenotype. Transcription factors seem to be susceptible to activation by titration. For example, in human gastric cancer, either haploinsufficiency or hypermethylation of the *RUNX3/AML-2* gene, coding for the DNA-binding component of a heterodimeric transcription factor, causes reduced protein expression that seems to play a role in early cancer development (11, 12). The homeoprotein OCT-3/4, a tumor suppressor in germ cell tumors, also undergoes gene dose-dependent inactivation (13). However, the relationship between LOH and reduced protein expression has not been shown. A recent study of *NKX3.1* expression in prostate cancer specimens reported that neither mRNA nor protein levels in histologic section correlated with Gleason grade or tumor stage (14). However, because we found that only 15% or less of such samples display loss of expression, the impact of haploinsufficiency on protein expression may be subtle and require quantitative assessment that controls for individual variation caused by biological differences or technical factors (5). We characterized the *NKX3.1* gene and protein expression in a cohort of human prostate cancers to determine the degree and mechanisms of inactivation of NKX3.1 in primary human prostate cancer.

## Materials and Methods

**Cell Culture.** Cultured cells were used to validate the *in situ* immunomicroscopic protein assay. LNCaP, TSU-Pr1, and TSU-Pr1(S11) cells were grown in IMEM medium supplemented with 20% fetal bovine

**Requests for reprints:** Edward P. Gelmann, Departments of Oncology and Medicine, Lombardi Comprehensive Cancer Center, Georgetown University, 3800 Reservoir Road, NW, Washington, DC 20007-2197. Phone: 202-444-2207; Fax: 202-444-1229; E-mail: Gelmanne@georgetown.edu.

serum (Life Technologies, Gaithersburg, MD), 400 g/mL gentamycin was added in flasks with TSU-Pr1 and TSU-Pr1(S11). LNCaP cells were grown in the presence or the absence of synthetic androgen R1881. LNCaP-R1881 cell were exposed to 1 g/mL of R1881 in standard FBS-IMEM for 24 hours. 293T embryonal kidney cells were grown in FBS-IMEM, split 1:5 and transfected with different amounts of an NKX3.1 expression vector using LipofectAMINE Reagent (Invitrogen, Inc., Carlsbad, CA). Cells were detached with a solution of 0.05% trypsin (Sigma-Aldrich, St. Louis, MO) and grown on chamber slides, fixed for 15 minutes in 4% formaldehyde in PBS at room temperature. Cells were permeabilized with 0.5% Triton X-100 in TBS [50 mmol Tris-HCl, 150 mmol NaCl, 0.1% $NaN_3$, (pH 7.6)] for 3 minutes.

**Microsatellite Analysis.** Genomic DNA was extracted from micro-dissected cancer and corresponding normal epithelial cells (see above) or uninvolved lymph nodes using the Qiagen DNA extraction kit. DNA was amplified by thermal cycler with nine microsatellite markers including D8S1734, D8S360, D8S1989, *NEFL*, D8S137, D8S87 (primers for which were obtained from the UniSTS database on the National Center for Biotechnology Information web site), and three unpublished markers CVMS9 (forward, 5′-GTG ATG AAT GAT CCT GCC ACA G-3′; reverse, 5′-ACA CTT CCA TTC ATG TTA GTC AC-3′), CVMS11 (forward, 5′ TGG TTT CCC GTA TAC CAA AGT C-3′; reverse, 5′-AGG AAA GGC CGT TTC CTC TG-3′), and CVMS12 (forward, 5′-GAG AGG AAC TTG AGA ACA GTG-3′; reverse, 5′ TCC ATG AGA CTG GTA CCT AG-3′).[1] The above mentioned markers are located on 8p21 within 12 Mbp from *NKX3.1*. Each PCR reaction was done using standard conditions of the Platinum Taq DNA polymerase kit in 10 L of reaction mixture containing 200 ng of template DNA and 0.25 L of each primer. The reaction mixture was denatured at 95°C and incubated for 29 to 31 cycles (denaturing at 94°C for 40 seconds, annealing at 57°C for 90 seconds, and extending 72°C for 90 seconds). Reaction products (8 L) were than electrophoresed in 8% polyacrylamide gel, stained with ethidium bromide, and visualized and imaged under UV illumination.

**Western Blotting.** Cells were suspended in lysis buffer [50 mmol Hepes (pH 7.5), 250 mmol NaCl, 0.5% Nonidet P40 with protease inhibitors], lysates were incubated on ice for 30 minutes and centrifuged at 13,000 × *g* for 15 minutes. The supernatant was collected and protein concentration was estimated with the Bio-Rad assay reagent. The protein was separated on a polyacrylamide gel (Invitrogen) followed by electrophoretic transfer to polyvinylidene difluoride membrane (Millipore, Bedford, MA) and blocking in 5% nonfat milk. NKX3.1 was detected on lysates of LNCaP cell with or without androgen treatment, TSU-Pr1(S11) and TSU-Pr1 cells using affinity-purified rabbit anti-NKX3.1 serum (1:3,000).

**Real-time PCR Assay.** The real-time quantitative PCR TaqMan assays were done on the Abi Prism 7700 Sequence Detection System equipment (Applied Biosystems, Foster City, CA). The primers and probe were selected for *NKX3.1* using Primer Express software (Applied Biosystems). The primer sequences were: forward, 5′-CGC AGC GGC AAG GC-3′; reverse, 5′-GGT GCT CAG CTG GTC GTT CT-3′. The probe sequence (CAG AGA CAG CGC GAC CCG G) was labeled at the 5′ end with the reporter molecule 6-carboxyfluorescein and at the 3′ end with the quencher BHQ-1. Amplification of commercially available endogenous control, β-actin (Applied Biosystems), was used to standardize the amount of sample DNA added. Dilutions of DNA from the cell line (LNCaP) were used to construct standard curves for the target gene and endogenous control. TaqMan Universal PCR Master Mix was combined with 100 ng of sample DNA, 900 nmol/L final concentration of primers, and 100 nmol/L final concentration of the probe. All samples were analyzed in replicates of four wells. Relative quantitation of the data from 7700 SDS was done using Sequence Detection System 2.1 Software (Applied Biosystems).

**Fluorescence *in situ* Hybridization.** Single cell nuclei were prepared from a 50-m paraffin section that was microdissected based on histologic analysis of an adjacent H&E-stained section. Nuclei were prepared using a modified Hedley method (15). A panel consisting of two probe sets was used: centromere 8 labeled with Spectrum Orange (red signal; Vysis, Inc./Abbott Laboratories, Downer's Grove, IL), and five fluorescein-labeled BAC clones (green signal) to detect *NKX3.1* loss: RP11-711D3 RP11-213G6, RP11-194F1, RP11-108E14, and RP11-219J21 (BACPAC Resources, Oakland, CA; Fig. 1*A*). RP11-213G6 contains the sequence of the *NKX3.1* gene. Cytospin slides were pretreated with RNase, followed by pepsin digestion and fixation in an ethanol series then denatured in 70% formamide/2× SSC for 2 minutes at 80°C. After overnight hybridization at 37°C,

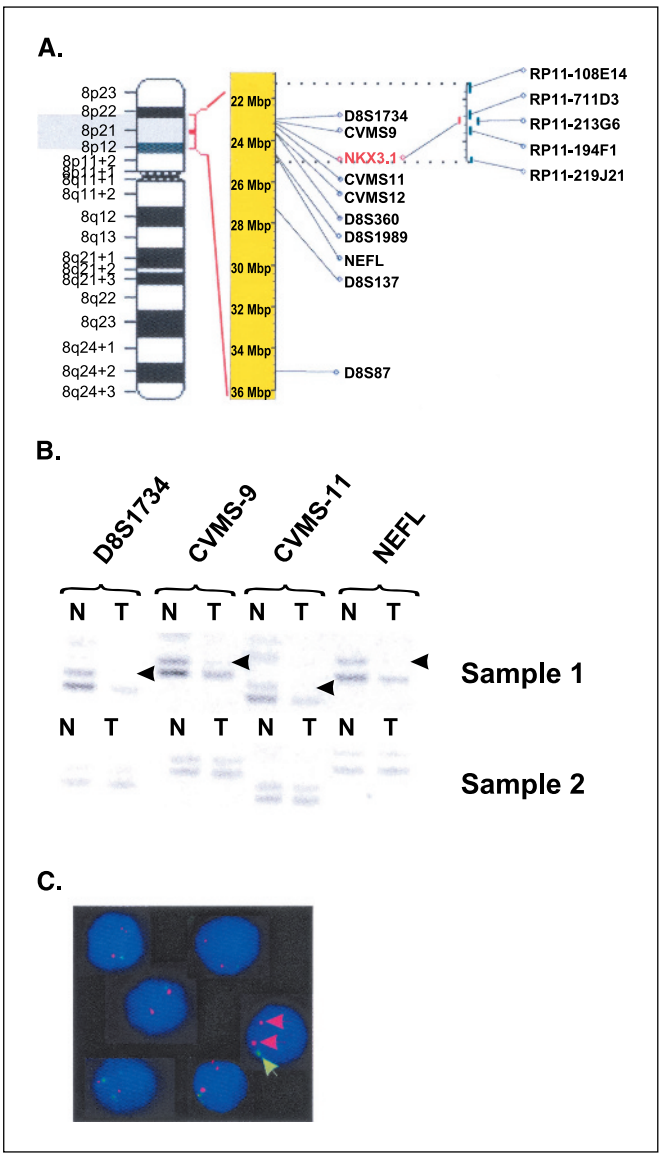


**Figure 1.** Analysis of *NKX3.1* copy number in primary prostate cancer tissues. Analysis of the *NKX3.1* gene in prostate cancers. *A,* map of chromosome 8 with location of the microsatellite markers used to determine LOH. *Right,* names and relative positions of the BAC clones used for interphase fluorescence *in situ* hybridization. *B,* example of results with four microsatellite markers used for LOH analysis. *Top,* samples analyzed with 8p21 LOH; *bottom,* samples with no LOH. *Arrows,* PCR transcripts representative of alleles that have been lost in tumor tissue. *C,* example of interphase fluorescence *in situ* hybridization done on nuclei prepared from paraffin-embedded tissue hybridized with chromosome 8 centromeric probe (*red*) and 8p21 probe panel (*green*). Note that the majority of nuclei in this sample showed allelic loss. Nuclei from normal cells are also seen.

[1] C. Vocke, National Cancer Institute, personal communication.

slides were washed thrice in 50% formamide/2× SSC at 42°C, and thrice in 1× SSC at 42°C. A blocking solution (4× SSC, 3% bovine serum albumin) was applied for 30 minutes at 37°C. The biotin-11-dUTP-labeled BAC probe was detected with Fluorescein-Avidin DCS (FITC-Avidin; Vector Laboratories, Inc., Burlingame, CA). Slides were washed in 4× SSC, 0.1% Tween 20 at 42°C, counterstained with 4′,6-diamidino-2-phenylindole, and embedded in antifade [200 mmol DABCO, 90% v/v glycerol, 20 mmol Tris-HCl (pH 8)] to reduce photobleaching. Scoring of cells and digital image acquisition were done using a 63× objective mounted on a Leica DMRBE microscope (Leica, Wetzlar, Germany) equipped with optical filters for 4′,6-diamidino-2-phenylindole, fluorescein isothiocyanate, SO, and a triple bandpass (Chroma Technologies, Brattleboro, VT), and a cooled charge-coupled device camera (Photometrics, Tucson, AZ). At least 200 nonoverlapping interphase nuclei were analyzed for each case. We defined a hemizygous deletion of the *NKX3.1* gene when more then 30% of the nuclei in a given case showed a ratio of NKX3.1-to-centromere signals of 1:2. Two control specimens were evaluated: nuclei prepared from a normal lymphocyte culture and nuclei prepared from a paraffin section obtained from a normal lymph node. In both cases, over 98% of the cells showed two signals for each of the two probes.

**Isolation and Treatment of DNA.** Genomic DNA of cell lines was isolated by using Puregene DNA isolation Kit (Gentra Systems, Minneapolis, MN). The QIAamp mini DNA kit (Qiagen, Inc., Valencia, CA) was used for purification of genomic DNA from 10 to 20 ten-micrometer sections from paraffin blocks. For bisulfite treatment, 2 μg DNA in 50 μL was denatured in 0.2 mol/L NaOH at 42°C for 10 minutes. Thirty microliters of fresh 10 mmol hydroquinone and 520 μL of 3 mol/L sodium bisulfite (Sigma) at pH 5.5 were added and mixed. The samples were covered with mineral oil and incubated at 50°C for 16 hours. Modified DNA was desalted with the Wizard DNA clean-up system (Promega, Madison, WI). For the denaturation step, 5.5 μL of 3 mol/L NaOH was added into 50 μL modified DNA solution and incubated at 37°C for 10 minutes, followed by ethanol precipitation with See DNA (Amersham Pharmacia Biotech, Piscataway, NJ) as coprecipitant.

**DNA Sequencing.** Bisulfite-modified DNA was amplified by nested PCR with NKX3.1-specific primers for individual regions containing CpG sites. First nested PCR primers for −1,056 to −687: sense, 5′-GGT ATT TTG AGA GGT TAA GGT AGG AGG A-3′; antisense, 5′-CCT TTA TCC ACA ATA ACC TAT TAA CTT TCC TTC C-3′. Second nested PCR primers for −1,056 to −687: sense, 5′-AGG AAA TCG AGG TTG TAG TGA GTT ATG A-3′; antisense, 5′-TCC CCA AAC ACA TAA CAT ACC ATC CT-3′. First nested PCR primers for −687 to −233: sense, 5′-GGT ATG TTA TGT GTT TGG GGA GGA AGG A-3′; antisense, 5′-CCC TAA AAA ATT CCT TCC CCA ATT CCC T-3′. Second nested PCR primers for −687 to −233: sense, 5′-GGA AGG AAA GTT AAT AGG TTA TTG TGG ATA AAG GA-3′; antisense, 5′-CTC CTT CCC CAA TTT CCT CTC CTT CT-3′. First nested PCR primers for −233 to 323: 5′-GGA GAG GGA ATT GGG GAA GGA G-3′; antisense: 5′-TCC CTA CAC CCC AAA CTC TAA AAA TCC-3′. The second nested PCR primers for −233 to +323: sense, 5′-AGG GAA TTG GGG AAG GAA TTT TTT AGG G-3′; antisense, 5′-CCT TAA ACT ACC CCC CTT CCC C-3′. The primers for +301 to +656: sense, 5′-GGG GAA GGG GGG TAG TTT AAG G-3′; antisense, 5′-CTT TAC TAA TCA ACC CCT ACT TTA TCA CT-3′. The primers for +627 to +1,172: sense, 5′-AGT GAT AAA GTA GGG GTT GAT TAG TAA AG-3′; antisense, 5′-CCC TTA TCT CTT TAA TAA ATA AAC AAA CAA CCC-3′. The primers to

**Table 1.** Primers for Methylation-Specific PCR

| CpG site | | | Sequence (5′-3′) |
|---|---|---|---|
| -1003 | First PCR | S | 5′- GGT ATT TTG AGA GGT TAA GGT AGG AGG ATT -3′ |
| | | AS | 5′- CCT ATT AAC TTT CCT TCC TCC CCA AAC ACA TA -3′ |
| | Second PCR | SU | 5′- TGA GTT ATG ATG GTA TTA TTG TAT TTT AGT TTG GGC - 3′ |
| | | SM | 5′- CAA ATT ACC AAC TAT TAA CAT ATA ACC CAT -3′ |
| | | AS | 5′- CAA ATT ACC AAC TAT TAA CAT ATA ACC CAT -3′ |
| -921 | First PCR | S | 5′- GGT ATT TTG AGA GGT TAA GGT AGG AGG ATT -3′ |
| | | AS | 5′- CCT ATT AAC TTT CCT TCC TCC CCA AAC ACA TA -3′ |
| | Second PCR | S | 5′- AGG AAA TCG AGG TTG TAG TGA GTT ATG A -3′ |
| | | ASU | 5′- CTA TAA CTA AAC TAA ACA ATA CCA TAA CAA CAA ACA -3′ |
| | | ASM | 5′- CTA AAC TAA ACG ATA CCG TAA CAA CAA ACG -3′ |
| -903 | First PCR | S | 5′- GGT ATT TTG AGA GGT TAA GGT AGG AGG ATT -3′ |
| | | AS | 5′- CCT ATT AAC TTT CCT TCC TCC CCA AAC ACA TA -3′ |
| | Second PCR | S | 5′- AGG AAA TCG AGG TTG TAG TGA GTT ATG A -3′ |
| | | ASU | 5′- TAA TCC AAC CGA TAC TAT AAC TAA ACT AAA CA -3′ |
| | | ASM | 5′- TAA TCC AAC CGA TAC TAT AAC TAA ACT AAA CG -3′ |
| -47 | First PCR | S | 5′- AGA AGG AGA GGA AAT TGG GGA AGG A -3′ |
| | | AS | 5′- CCT CCC TCT AAC TCT AAC TCT AAC TCC -3′ |
| | Second PCR | S | 5′- AGG GAA TTG GGG AAG GAG AGG GAA T -3′ |
| | | ASU | 5′- CAC CCA CCC AAC CCA CAC CA -3′ |
| | | ASM | 5′- CCC GCC CGA CCC GCA CCG -3′ |
| 872 | First PCR | S | 5′- AGT GAT AAA GTA GGG GTT GAT TAG T -3′ |
| | | AS | 5′- CAT TCA TTT ACT AAA AAT CAT CAA AAA CCC -3′ |
| | Second PCR | S | 5′- AGT GAT AAA GTA GGG GTT GAT TAG T -3′ |
| | | ASU | 5′- CCC AAA AAA ACC AAA CCA AAA AAC ATC CA -3′ |
| | | ASM | 5′- CCC AAA AAA ACC AAA CCA AAA AAC ATC CG -3′ |
| 938 | First PCR | S | 5′- AGT GAT AAA GTA GGG GTT GAT TAG T -3′ |
| | | AS | 5′- CAT TCA TTT ACT AAA AAT CAT CAA AAA CCC -3′ |
| | Second PCR | S | 5′- GAA GAG GGA ATT AAA GTT TAG AAT GAG T -3′ |
| | | ASU | 5′- TAT AAA AAT TCT AAA TCT ATA TAC TAA AAA AAA ACG -3′ |
| | | ASM | 5′- TAT AAA AAT TCT AAA TCT ATA TAC TAA AAA AAA ACA -3′ |

Abbreviations: S/AS, sense/antisense primers; ASU/ASM, antisense unmethylated/methylated primers.

detect the AR gene after bisulfite modification: sense, 5′-TGG TTT AGG AAA TTA GGA GTT ATT TAG G-3′; antisense, 5′-TCC CTT CGA CTC CTA TAC AAC ACT A-3′.

**Methylation-Specific PCR.** Bisulfite-modified DNA from cell lines was amplified directly and from paraffin-embedded tissues by nested PCR using methylation-specific PCR primers. Six CpG sites were selected to study their methylation status based on the results of bisulfite sequencing. All the primers used in methylation-specific PCR are listed in Table 1. PCR conditions for first PCR were 95°C for 15 minutes, 94°C for 1 minute, 52°C for 1 minute, 72°C for 45 seconds, 33 to 36 cycles; 72°C for 10 minutes, then at 4°C. One to five microliters of the first PCR product was taken as a template for the second reaction in a final volume of 50 μL. PCR conditions for the second PCR were 95°C for 15 minutes, 94°C for 1 minute, 53°C for 1 minute, and 72°C for 45 seconds. PCR was run for 16 to 32 or 26 to 38 cycles depending on the efficiency of primers in amplification; 72°C for 10 minutes, then at 4°C. PCR products were run on 1.6% agarose gel in 1× Tris-borate EDTA buffer with EB (0.4 μg/mL). Based on the relative intensities of "methylated" (M) compared with "unmethylated" (U) signals in the PCR reactions stopped after different cycles, we determined whether there was a greater degree of methylation in malignant compared with nonmalignant cells.

**Paraffin-Embedded Tissues.** Paraffin-embedded prostate cancer specimens were obtained from the Lombardi Comprehensive Cancer Center Histopathology and Tissue Shared Resource. All samples were from radical prostatectomies done at Georgetown University Hospital or the Washington DC Veterans Affairs Hospital and provided to the Shared Resource with the approval of the respective Institutional Review Boards. Pathology reports were retrieved for 43 specimens. The ages ranged from 48 to 72. The distribution of histologic grades taken from review of H&E sections at the time of analysis were Gleason grades 3–30, 4–16, and 5–2. T stages ranged from $pT_{2a}$ to $pT_{4a}$. None of the 43 cases for which we retrieved pathology reports had had lymph node involvement and thus were all $N_0$.

Multiple parallel 4-μm sections were cut with a Leitz microtome. The sections were deparaffinized with xylene and hydrated through graded alcohols into water. One section from each tissue block was stained with H&E. The remaining sections were stored at room temperature for immunofluorescence staining. Areas of tumor and nonmalignant epithelial

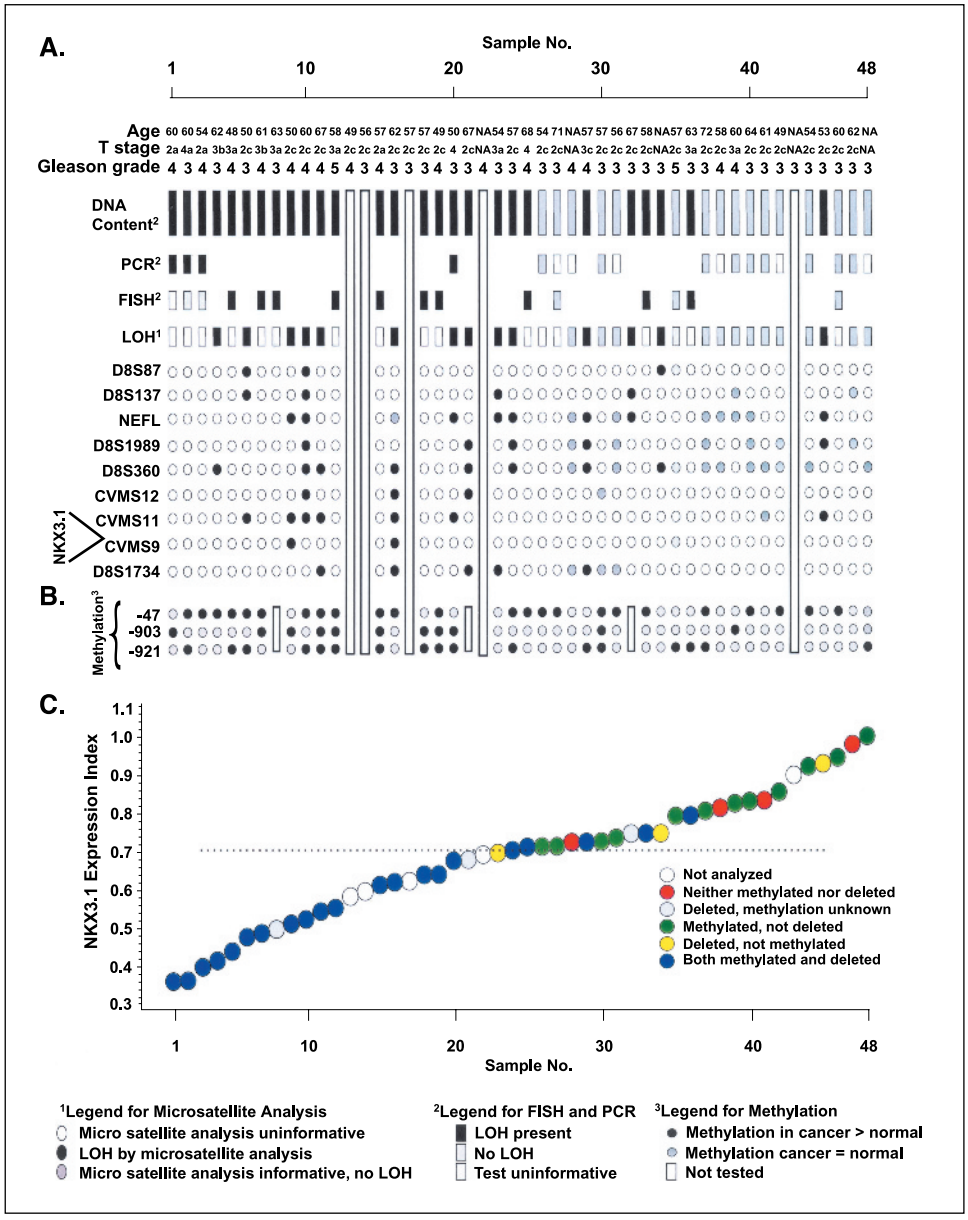


**Figure 2.** Summary of genotypic, methylation, and expression data. *A,* results for individual microsatellite markers (*bottom*). Conclusions of the microsatellite analysis are indicated in the row designated "LOH". Results of fluorescence *in situ* hybridization analysis are shown above the LOH summary. Lastly, quantitative PCR results are summarized. The status of each tissue with regard to *NKX3.1* copy number (*top*). *B,* methylation of each of three CpG sites is shown. Samples are aligned with the individual data in *A*. *C,* correlation between *NKX3.1* expression and gene alteration. Each circle represents an individual tumor arranged by NKX3.1 staining index. Samples are aligned with the individual data in *A* and *B*.

cells were marked on H&E sections and correlated with the sections analyzed by immunomicroscopy. Microdissection was done from paraffin blocks based on analysis of an H&E-stained section showing at least 90% cancer cells for areas of malignant tissue and no visible malignant cells, but a high concentration of glands in regions of nonmalignant tissue. We also avoided regions of inflammation or atrophy in selecting the benign epithelial cells for analysis. The fidelity of microdissection was confirmed by repeat sectioning of the dissected block. All histologic analyses were confirmed by one of us (E.P. Gelmann) with extensive experience with prostate pathology (16). Pathologic review was provided by the director of the Histopathology and Tissue Shared Resource. Prostates from wild-type, *Nkx3.1*$^{+/-}$, and *Nkx3.1*$^{-/-}$ mice (8) were obtained from Cory Abate-Shen (University of Medicine and Dentistry, New Brunswick, NJ) and stained with our rabbit anti-human NKX3.1 polyvalent affinity-purified antiserum similarly to staining of human tissues.

**Antibody Staining.** Antigen retrieval was done in citrate buffer using a Black & Decker vegetable steamer. Blocking of nonspecific binding sites was done with goat serum in TBS (1:70) for 30 minutes. Histone expression was detected with mouse monoclonal anti-histone antibodies (1:1,000, Santa Cruz Biotechnology, Santa Cruz, CA) followed by secondary affinity-purified biotinylated horse anti-mouse antibody (1:200, Vector Laboratories, Burlingame, CA) and revealed with Texas red-avidin (1:200, Vector Laboratories). NKX3.1 was detected with affinity-purified rabbit anti-NKX3.1 serum (1:1,000; ref. 5) and fluorescein-conjugated goat anti-rabbit antibody (1:200, Vector Laboratories). For murine prostate samples, blocking was done with horse serum in TBS (1:70). Histone expression was detected with goat anti-histone antibodies (1:500, Santa Cruz Biotechnology) followed by secondary biotinylated horse anti-goat antibody and revealed with Texas red-avidin (1:200, Vector Laboratories). NKX3.1 was detected with rabbit anti-NKX3.1 antibody as described above and revealed with affinity-purified fluorescein-conjugated donkey anti-rabbit antibody (1:200, Pierce, Rockford, IL).

**Image Acquisition and Analysis.** All images were collected on Olympus IX 70 confocal inverted microscope with laser scanning unit and a 60× NA oil lens (Carl Zeiss, Thornwood, NY). Samples were excited with argon laser 488 nm and krypton laser 568 nm. Areas imaged were randomly chosen while visualizing histone staining with Texas red, common to all cells, to eliminate sampling bias. Only luminal epithelial cells and malignant cells were chosen for assay. The intensity of the obtained signal was calibrated to avoid saturation of signal, using hue-saturation-intensity channel of Fluoview 2.1 software (Olympus, Melville, NY). Images were saved as 24-bit color files. Obtained images were analyzed using the MetaMorph software (Universal Imaging Corporation, Downingtown, PA). Computer-assisted tracing of nuclei on randomly chosen cells ($n$ = 50) from each cell type on the slide was done while visualizing cells for Texas red (histone) staining to decrease sampling bias. After background subtraction and adjustment of threshold image intensity of fluorescein isothiocyanate (NKX3.1) and Texas red (histone) staining was calculated using the average intensity–measuring tool of the software. Data was expressed in pixels and stored for further statistical analysis. Analysis of staining intensity for both NKX3.1 and histone H1 in each cell type showed that SD were <10% within each cell type of each sample. Data for each human tissue was expressed as an index of NXK3.1 expression calculated as the ratio of NKX3.1 (cancer)/NKX3.1 (normal) divided by histone H1 (cancer)/histone H1 (normal).

**Tissue Microarray.** We have previously constructed a prostate cancer prognostic tissue microarray from 561 prostate cancer patients, that was described and validated by analysis of Gleason grading in the microarray samples (17). The microarray contains tissues from a cohort of 750 prostatectomy patients treated at a single institution and followed for a median of 6.2 years from the date of surgery (16). NKX3.1 staining of the array and visual scoring was done as previously described (5).

**Statistical Methods.** All statistical tests used (one-way and two-way ANOVA, linear regression models, correlation tests, and $t$ test) were done using SAS (SAS Institute, Inc., Cary, NC) and Splus (MathSoft, Inc., Cambridge, MA) software. Plots were constructed using SigmaPlot software (Statistical Package for the Social Sciences, Inc., Chicago, IL).

## Results

***NKX3.1* Gene Copy Number.** From a cohort of 48 specimens that were analyzed for NKX3.1 expression (see below) we analyzed normal and cancer cell DNA from 43 specimens with sufficient material for LOH of a variety of microsatellite markers in the 8p21.2 region (Fig. 1*A* and *B*). Details of the samples including age, pathologic stage, and Gleason grade are shown in Fig. 2*A* (*top*). Twenty-seven tested specimens were found to be informative; of those, 14 had LOH (Fig. 2*A*). Sixteen samples for which microsatellite analysis had been uninformative were analyzed by interphase fluorescence *in situ* hybridization using BAC clones that spanned ~4 Mbp of the 8p21 chromosomal region and included *NKX3.1* (Fig. 1 *A* and *C*). Ten specimens were found to have undergone deletion of 8p21 by this approach (Fig. 2*A*). Lastly, of the remaining 18 specimens in which we had not detected 8p21 deletion by either microsatellite analysis or fluorescence *in situ* hybridization, and in one sample which was found to have undergone deletion of 8p21 by microsatellite analysis, we assayed *NKX3.1* DNA content in microdissected tissue by quantitative PCR. Nine specimens had a ratio of *NKX3.1* DNA in tumor and normal regions of 1.0 ± 0.1, six specimens had ratios of 0.8 ± 0.1, the remaining four samples had ratios < 0.7 (0.6, 0.64, 0.4, and 0.58) and were deemed to have unequivocal *NKX3.1* DNA deletion. One sample (#20 in Fig. 2*A*) in which we had detected LOH by microsatellite analysis was also analyzed by quantitative PCR and had a *NKX3.1* tumor/normal ratio gene content of 0.58. Overall, 27/43 (62.8%) samples were determined to have either 8p21 deletion or reduced *NKX3.1* DNA content.

**NKX3.1 Methylation.** To identify candidate CpG islands that are associated with *NKX3.1* gene expression, we first analyzed *NKX3.1* methylation in LNCaP prostate cancer cells that express NKX3.1 protein and in PC-3 and DU-145 cells that do not (5). The region of *NKX3.1* from −1,100 to +1,250 contains 150 CpG dinucleotides, 51 in the 5′ upstream segment, 39 in exon I, and 60 in intron I. Of the 150 CpG dinucleotides studied, 28 were found by DNA sequencing to be methylated or partially methylated in prostate cancer cell lines (Fig. 3*A*). The frequencies of CpG dinucleotide methylation were 18/150 in both PC-3 cells and DU-145 cells, but 10/150 in LNCaP cells. We found no contiguous regions of CpG island methylation. Consistent with this finding, treating PC-3 or DU-145 cells with 5-azacytidine, trichostatin A, or both had no effect on either *NKX3.1* methylation, mRNA expression, or NKX3.1 protein expression under conditions where androgen receptor expression was activated (data not shown; ref. 18). We concluded that there was no evidence of CpG island methylation in *NKX3.1* and that inhibition of either methylation or histone deacetylation did not activate *NKX3.1* expression in prostate cancer cell lines.

We also analyzed *NKX3.1* gene methylation in tissues. We could not obtain sufficient DNA from the 48 prostate cancer tissue blocks to perform sequence analysis of *NKX3.1* so we analyzed selected CpG dinucleotides by methylation-specific PCR. The choice of sites to be analyzed was instructed by the data obtained with the cell lines. We chose −1,003 located in an Sp1 bind site (−1,006 to −1,001); −921 fully methylated in all three prostate cancer cell lines; −903 completely methylated in PC-3 cells and DU-145 cells, but partially methylated in LNCaP cells; −47 located in a second Sp1 binding site and fully methylated in PC-3 and DU-145 cells, but not methylated in LNCaP cells; +872 methylated only in DU-145 cells and not in PC-3 or LNCaP cells; +938 methylated in the three

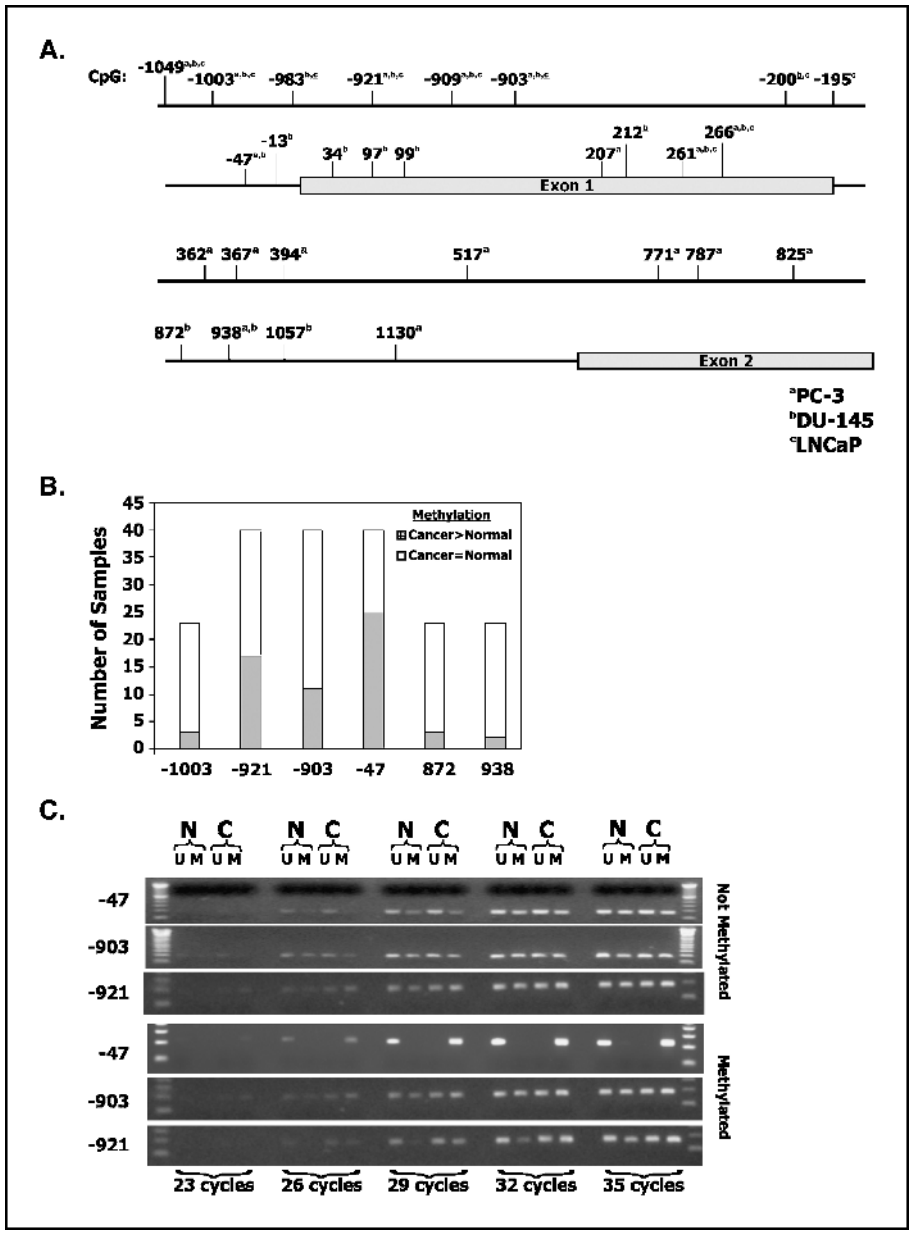


**Figure 3.** Methylation of *NKX3.1* in cell lines and tissues. Methylated CpG dinucleotides of NKX3.1 in prostate cancer cell lines. *a,* PC-3; *b,* DU-145; *c,* LNCaP; *underlined superscripts,* partially methylated. *B,* methylation of six selected *NKX3.1* CpG sites in microdissected prostate cancer tissues. Samples were found either to have similar methylation in malignant and nonmalignant regions or to have increased methylation at one or more CpG sites in malignant regions. *C,* example of methylation analysis by methylation-specific PCR. *Top,* equal degrees of methylation in normal and cancer cells at all three sites. *Bottom,* preferential methylation of malignant cells at −47 and −921. Note that the ratio of unmethylated to methylated DNA at −921 is greater for normal cells than for cancer cells.

cell lines and located in intron I. We analyzed 22 samples for methylation at all six sites and found that for three, −1,003, +872, and +938 there was rarely any difference between malignant and adjacent normal tissue. On the other hand, CpG sites at −921, −903, and −47 often displayed a greater degree of methylation in cancer than nonmalignant tissue (Fig. 3*B*). An additional 18 samples for which we had sufficient DNA were analyzed for methylation at those three sites. Examples of methylation-specific PCR results for one sample that had no preferential methylation of cancer and for one that did are shown in Fig. 3*C*. The results of methylation analysis of three CpG sites in 40 tissue specimens are shown in Fig. 2*B*.

**NKX3.1 Expression.** To measure relative expression of NKX3.1 protein in nonmalignant and malignant cells, we developed a protocol whereby malignant and nonmalignant cells could be assayed for expression of NKX3.1 and a control nuclear protein on a single paraffin section. Two-color fluorescence was used to measure relative NKX3.1 expression in cancer cells and adjacent nonmalignant prostatic epithelium simultaneously with histone H1 expression, the internal control for nuclear staining. Because of the potential technical artifacts in fluorescence intensity 7measurements, we validated the assay with cultured cells expressing different amounts of NKX3.1. First we analyzed the expression of a reference nuclear protein, histone H1, and showed that its expression was correlated with cellular DNA content, as shown by more intense staining in LNCaP cells (DNA content, 1.8; measured by flow cytometry of propidium iodide-stained cells) than in TSU-Pr1 and TSU-Pr1(S11) cells (DNA content, 1.5). The ratio of histone H1 expression in LNCaP/TSU-Pr1 is 1.46; and the ratio of DNA contents is 1.2 (Fig. 4*A*). Quantitation of NKX3.1 expression using confocal microscopy was validated with LNCaP prostate cancer cells that express NKX3.1 in an androgen-regulated

manner, TSU-Pr1 transitional carcinoma cells that do not express NKX3.1, and derivative TSU-Pr1(S11) cells engineered to express NKX3.1 (5). NKX3.1 staining was the highest in LNCaP cells exposed to the androgen R1881 [mean, 175; 95% confidence interval (CI) 4.1; ref. 19], followed by LNCaP cells (mean, 100; 95% CI, 3.14), then TSU-Pr1(S11) (mean, 70; 95% CI 2.3), and was close to background in TSU-Pr1 (mean, 0). The confocal assay of NKX3.1 expression correlated well with the results of a Western blot (*bottom*, Fig. 4*B*). An example of the photomicrographic images of the cultured cells analyzed in Fig. 4*A* and *B* is shown in Fig. 4*C*. Next, we transfected 293T embryonal kidney cells with different amounts of an NKX3.1 expression vector and found that transfected cells expressed protein in proportion to the amount of DNA transfected and that the relationship between the mass of the transfected plasmid and the expression index was linear (Fig. 4*D*).

To validate the immunofluorescent measurements on tissue sections, we used prostates from gene-targeted mice (8). For analysis of these tissues, we did not have cells with different *Nkx3.1* gene content in the same section that would have been the equivalent of malignant and nonmalignant tissues. However, by setting the background fluorescence of $Nkx3.1^{-/-}$ samples at zero, we determined the Nkx3.1 expression levels in heterozygous and wild-type mice compared with histone expression. Nkx3.1 expression index in heterozygous mice gave a relative value of 2.9 and in wild-type mice a relative value of 4.5 (Fig. 4*E*). The result showed that we were able to detect differences in protein expression based on gene copy number and suggested that there may have been compensatory overexpression of Nkx3.1 from the residual allele in the heterozygous mice.

Forty-eight paraffin-embedded prostate cancer specimens were analyzed for NKX3.1 expression in adenocarcinoma and adjacent normal epithelial cells. In addition, a second paraffin block was included from five cases and analyzed in a blinded fashion to assess the reproducibility of our assay and uniformity of NKX3.1 expression within an individual cancer. The ratio of histone H1 staining in malignant and normal cells ranged between 0.93 and 1.08 for all 48 samples tested. In contrast, the ratio of NKX3.1 expression in malignant to nonmalignant epithelial cells was significantly less then 1 when calculated directly or when normalized to histone expression (mean, 0.68; 95% CI, 0.05; Fig. 5*A*). An example of a confocal image is shown in Fig. 5*B*. For the five cases from which we assayed two separate paraffin blocks, the correlation between NKX3.1 expression levels was high (correlation coefficient, 0.99). We also examined the hypothesis that *NKX3.1* down-regulation is one of the earliest lesions in prostate cancer by assaying expression in high-grade

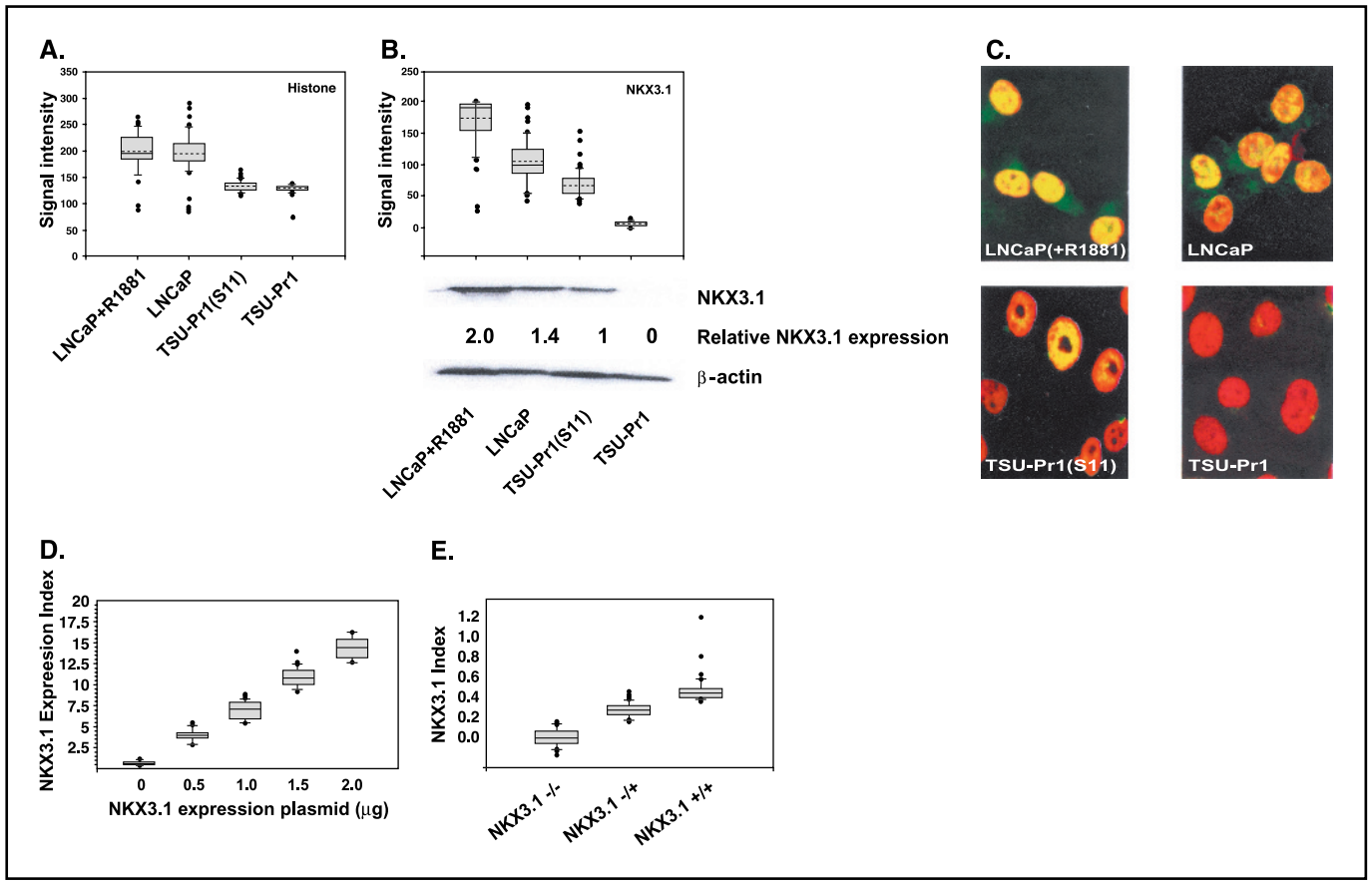


**Figure 4.** Validation of protein expression assay. *A,* assay of 50 to 100 cells of each type for histone H1 expression. *Horizontal solid line,* median; *dotted line,* mean value. *Shaded box,* 75% percentile range, with 95% error bars and outliers as dots. *B,* assay of nuclear staining for NKX3.1. Western blot of total cellular proteins for NKX3.1 and β-actin is shown below the plot. Values indicate the relative amounts of NKX3.1 normalized to β-actin. *C,* confocal images of cells used for quantitation in *A* and *B*. The merging between *green* and *red* in the nuclei appears as *yellow* in the image. The depth of the *yellow* color reflects the NKX3.1 staining compared with histone and is converted by the image analyzer to *green*. *D,* confocal immunomicroscopic assay of NKX3.1 expression in HEK293T cells transfected with increasing amounts of NKX3.1 expression plasmid. *E,* Nkx3.1 expression in prostate tissues from gene-targeted mice.

prostatic intraepithelial neoplasia as well as in invasive cancer. We identified high-grade prostatic intraepithelial neoplasia in 12 of the 48 samples, and these cells were also found to have a reduction in NKX3.1 expression similar to the corresponding invasive cancer cells (Fig. 5*C*). In a linear model, the regression coefficient was $\beta = 0.7079$ with a $P$ value of $< 0.0178$.

We compared the NKX3.1 expression levels to the gene deletion and CpG methylation data (Fig. 2*C*). One-way ANOVA showed strong correlation between loss of 8p21 or *NKX3.1* and NKX3.1 expression ($P < 0.0001$). For the group of tumors for which we were not able to show DNA loss, the mean NKX3.1 index was 0.83 (SE, 0.09), compared with 0.6 (SE, 0.15) for the group with LOH. The combined effects of gene deletion and methylation had a more profound effect on reducing NKX3.1 expression than either alone. Two-way ANOVA showed that DNA loss was the dominant factor that influenced NKX3.1 expression ($P = 0.0001$), whereas the effect of methylation was marginal ($P = 0.07$). However, NKX expression decreased in relation to the number of sites methylated of the three sites analyzed ($P = 0.0073$ if we use one-way ANOVA). The NKX3.1 expression indices followed a normal distribution as indicated by a QQ plot on which the relationship between the quantiles of expression values and a standard normal random variable is approximately linear. To confirm this observation, Kolmogorov-Smirnov goodness-of-fit test gave a $k_s$ value of 0.078 ($P = 0.5 > 0.05$), therefore, we could not reject the hypothesis that the NKX3.1 index was normally distributed. We were unable to detect either *NKX3.1* gene methylation or deletion in four samples.

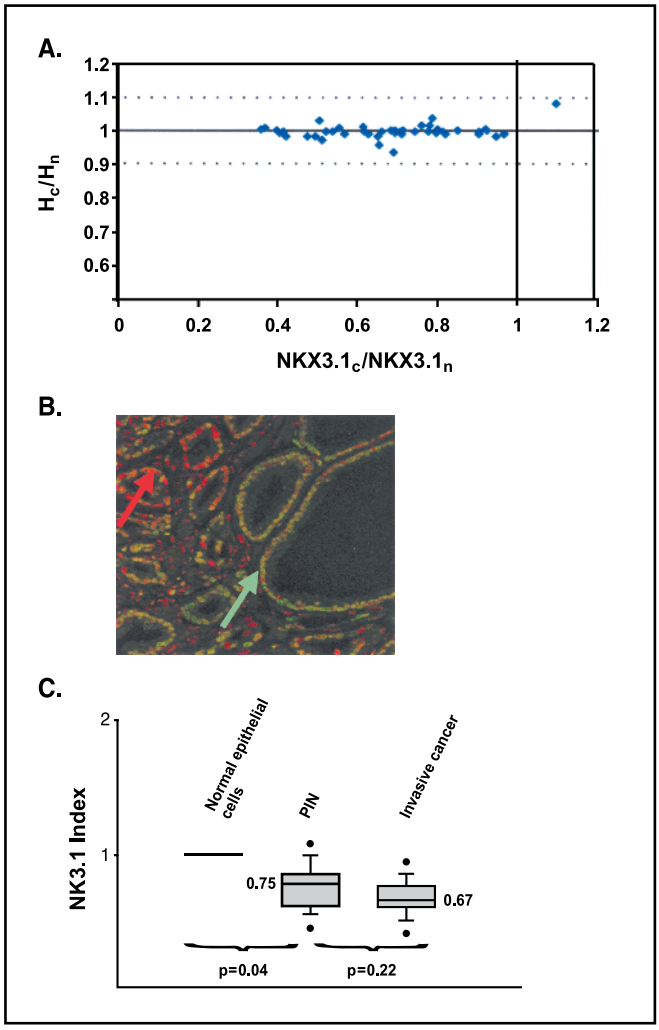


**Figure 5.** NKX3.1 expression in malignant prostate epithelium. NKX3.1 expression in prostate cancer tissues. *A,* plot of NKX3.1 index versus histone expression index in 48 prostate cancer cases. *B,* photomicrograph of two-color confocal image of nonmalignant (*green arrow*) and adjacent malignant cells (*red arrow*) in a tissue stained for histone H1 (*red*) and NKX3.1 (*green*). *C,* NKX3.1 staining in high-grade prostatic intraepithelial neoplasia and adjacent invasive cancer in 12 specimens.

The current cohort of 48 samples was not expected to be large enough to correlate the degree of NKX3.1 expression and clinical parameters such as Gleason grade. For the sake of completeness we conducted statistical analyses for NKX3.1 expression and age. Statistical analysis for NKX3.1 expression and age or Gleason score showed nonsignificant trends toward lower expression of NKX3.1 in tumors from younger patients ($P = 0.39$ by simple linear model) and higher Gleason score ($P = 0.37$ by one-way ANOVA). Tumor stage was randomly distributed across the NKX3.1 expression range. The only statistically significant correlation was found for Gleason grade. When Gleason grade was treated as an independent variable and NKX3.1 as a dependent variable, one-way ANOVA analysis showed reverse correlation ($P = 0.032$). As there were only two patients with grade 5 tumors, further analyses were done on patients with grade 3 versus combined grade 4 and 5 tumors. The mean NKX3.1 expression index for patients with Gleason grade 3 was 0.73 ($n = 30$) and for patients with Gleason grade 4 or 5, it was 0.61 ($n = 18$), the 95% confidence interval for their difference in means (0.032-0.213) did not include zero. Therefore, we can conclude that the mean NKX3.1 indexes were significantly different between these two groups ($P < 0.01$, Welch's two-sample $t$ test).

Recently, NKX3.1 mRNA and protein expression were analyzed in a larger cohort and was shown not to correlate with histologic grade or clinical stage (14). To investigate this relationship in a well-characterized cohort of prostatectomy samples in a prostate cancer tissue microarray, we did an analysis of 561 prostate cancer samples for qualitative loss of NKX3.1 expression (see Materials and Methods). We previously had shown that about 10% to 15% of primary prostate cancers had lost conventional qualitative immunohistochemical staining for NKX3.1 (5). We analyzed NKX3.1 expression by staining a tissue microarray of primary prostatectomy samples from 561 men with up to 30 years of follow-up (16, 17). Only 26 samples (4.6%) showed complete qualitative loss of NKX3.1 expression as previously defined. Among this group, there was no difference in disease-free or overall survival compared with the patients with detectable NKX3.1 expression. Therefore, our results are consistent with recently published findings that loss of NKX3.1 expression does not have major prognostic significance in primary prostate cancer patients (14).

## Discussion

Our data show that *NKX3.1* was deleted in about 63% of the samples studied. This fraction is lower than the frequency suggested by the 8p21 LOH analysis reported previously (3). Nevertheless, in the absence of somatic mutations that are not found in human cancer specimens, this is the first analysis that focuses on the copy number of this suppressor gene in human cancer (6, 7). It is possible that our survey underestimated the frequency of LOH because we would have missed smaller deletions, particularly those affecting the 3′ end of the *NKX3.1* gene that were not assayed in the real-time PCR analysis. The two coding exons of

*NKX3.1* are located at the 5′ end of the gene as predicted by nucleotide sequencing. No targeted somatic disruption of these two exons has been identified in cancer tissues (6, 7); however, the 3′ end of the gene that codes for noncoding sequences that comprise the major portion of a 4.2 kb mRNA have not been analyzed in prostate cancer specimens. The potential influence of the 3′ noncoding exons on *NKX3.1* mRNA stability and protein expression has not yet been studied. Our expectation in initiating this study was that reduced *NKX3.1* gene copy number would be sufficient to reduce protein expression. In *Nkx3.1* gene-targeted mice, we found that Nkx3.1 expression was reduced, but not by fully half the level of expression in wild-type tissues. Loss of an allele may be compensated by increased expression from the residual allele. In human specimens, we found a much wider range of expression levels across a binomial distribution around the median 0.7. Because we were not able to find evidence of LOH in all the specimens, both gene deletion and other factors influenced the expression of *NKX3.1* in prostate cancer tissues, suggesting a complex set of events can result in partial inactivation of this suppressor protein. One factor that influenced gene expression was methylation detected at very few sites upstream from the protein coding region.

Quantitative analysis of protein expression in histologic samples is difficult. We carried out expression analysis to understand the degree of NKX3.1 down-regulation in prostate cancer. Although there are concerns about the accuracy of immunofluorescence microscopy to assay protein levels, there are validated approaches to this problem (20). Moreover, we validated our internally controlled assay using both cultured cells and fixed tissues in order to show that we could detect quantitative differences of NKX3.1 expression in a reproducible fashion.

Gene methylation has been implicated in the silencing of tumor suppressor genes (21). Despite a large number of CpG sites in the 5′ untranslated and first exon regions of *NKX3.1* we found no wholesale CpG island methylation in cell lines that do not express NKX3.1 protein and have down-regulated mRNA expression 50- to 100-fold.[2] We were unable to affect methylation of the *NKX3.1* upstream region by exposing cells to 5-azacytdine, an inhibitor of DNA *N*-methyltransferase even in combination with trichostatin A, an inhibitor of histone deacetylase. Interestingly, we found tumor-specific methylation at selected CpG dinucleotides that correlated to some degree with protein expression and combined with LOH was a strong predictor of low NKX3.1 expression. However, the significance of this finding, beyond the correlation with LOH in tissues with lower levels of protein expression, is unclear. Not surprisingly, samples with methylation but no detectable LOH had a mean NKX3.1 expression index of 0.83 $\pm$ 0.09, identical to the mean expression index of samples with no detectable methylation or LOH (0.83 $\pm$ 0.09). Moreover, in human tissues *NKX3.1* mRNA expression by *in situ* hybridization correlates with immunohistochemical assay for protein expression (14). Expression of *NKX3.1* mRNA in human prostate cancers was found not to be qualitatively different from expression in adjacent normal cells (7, 22). However, analysis of *NKX3.1* mRNA from human prostate cancers by more quantitative methods has not been reported. Interestingly, in prostate tumors of $Nkx3.1^{+/-}$, $Pten^{+/-}$ or $Pten^{+/-}$ mice Nkx3.1 protein expression is not found in nascent tumors despite the persistence of *Nkx3.1* mRNA as detected by *in situ* hybridization (23). We can only speculate that the limited DNA methylation we have found has some yet unexplained function in the regulation of gene expression.

Consistent with the notion that reduced *NKX3.1* activity is an early critical event in the genesis of sporadic prostate cancer, we have shown that most primary cancer tissues have decreased expression of the protein. Allelic deletion was the primary genetic alteration that correlated with decreased NKX3.1 expression, although methylation also correlated with decreased expression in a subset of cases and was found in most cases where the gene was deleted. Interestingly, although 19 of the 48 cases had NKX3.1 expression indices within 10% of the median, the remainder varied up to 50% above or below the median. This suggests that a variety of factors influence the expression of NKX3.1 in prostate cancer cells even when one allele is deleted. The mean NKX3.1 expression index in samples with documented loss on 8p21 but no methylation was 0.76 $\pm$ 0.09, whereas the mean expression index with samples where both methylation and LOH were detected was 0.55 $\pm$ 0.13. Both of these indices exceed the hypothetical level of 0.5 that might result from loss of one of two gene copies, suggesting that the remaining allele does increase expression to compensate for haploinsufficiency as suggested in the mouse model.

We propose that variations in NKX3.1 expression are pathogenic in the human prostate and contribute to early malignant transformation. The finding that NKX3.1 expression was also reduced in high-grade prostatic intraepithelial neoplasia is consistent with this hypothesis. The data are somewhat tempered by the fact that we analyzed prostatic intraepithelial neoplasia in the same tissues where invasive cancer was present. An analysis of high-grade prostatic intraepithelial neoplasia in prostates that lack cancer has not been done, but is more problematic because the quantity of tissue is often limited in the absence of radical prostatectomy. The capacity of Nkx3.1 to control cell growth and differentiation in the murine prostate and findings that *Nkx3.1* deletion cooperates with loss of *Pten* and *p27* to potentiate prostate tumorigenesis support the hypothesis that alterations of NKX3.1 expression affect human prostate carcinogenesis. NKX3.1 is a homeodomain protein that has a broad range of molecular interactions. These include direct binding to DNA (24) and interaction with other transcription factors such as serum response factor (25, 26). Protein association studies have also suggested that NKX3.1 plays a role in DNA replication and activation of the transcriptional complex.[3] Further studies will clarify whether NKX3.1 has a role in oncogenic pathways involving cell growth, apoptosis, cell cycle control, or DNA repair. These studies will also provide a foundation for therapeutic applications targeted at increasing NKX3.1 activity or protein levels in early stage prostate cancer.

## Acknowledgments

Received 7/28/2004; revised 11/15/2004; accepted 11/30/2004.

**Grant support:** USPHS grant ES09888 to E.P. Gelmann and Department of Defense grant DAMD17-02-1-0058 to W-X. Huang.

The costs of publication of this article were defrayed in part by the payment of page charges. This article must therefore be hereby marked advertisement in accordance with 18 U.S.C. Section 1734 solely to indicate this fact.

We thank Janice D. Rone and Nicole White for technical assistance. Confocal microscopy was supported by the Microscopy and Imaging Shared Resource. Tissues came from the Histopathology and Tissue Shared Resource of the Lombardi Comprehensive Cancer Center. Bhaskar Kallakury (Department of Pathology, Georgetown University) provided pathology review and consultation. We thank Cory Abate-Shen and Michael Shen for murine tissues.

[2] W-X. Huang and E.P. Gelmann, unpublished data.
[3] N. Ahronovitz and E.P. Gelmann, unpublished observations.

## References


1. Bova GS, Carter BS, Bussemakers JG, et al. Homozygous deletion and frequent allelic loss of chromosome 8p22 loci in human prostate cancer. Cancer Res 1993;53:3869–73.
2. Emmert-Buck MR, Vocke CD, Pozzatti RO, et al. Allelic loss on chromosome 8p12-21 in microdissected prostate intraepithelial neoplasia. Cancer Res 1995;55: 2959–62.
3. Vocke CD, Pozzatti RO, Bostwick DG, et al. Analysis of 99 microdissected prostate carcinomas reveals a high frequency of allelic loss on chromosome 8p21-22. Cancer Res 1996;56:2411–6.
4. Swalwell JI, Vocke CD, Yang Y, et al. Determination of a minimal deletion interval on chromosome band 8p21 in sporadic prostate cancer. Genes Chromosomes Cancer 2002;33:201–5.
5. Bowen C, Bubendorf L, Voeller HJ, et al. Loss of NKX3.1 expression in human prostate cancers correlates with tumor progression. Cancer Res 2000;60: 6111–5.
6. Voeller HJ, Augustus M, Madlike V, Bova GS, Carter KC, Gelmann EP. Coding region of NKX3.1, prostate-specific homeobox gene on 8p21, is not mutated in human prostate cancers. Cancer Res 1997;57:4455–9.
7. Ornstein DK, Cinquanta M, Weiler S, et al. Expression studies and mutational analysis of the androgen regulated homeobox gene nkx3.1 in benign and malignant prostate epithelium. J Urol 2001;165:1329–34.
8. Bhatia-Gaur R, Donjacour AA, Sciavolino PJ, et al. Roles for Nkx3.1 in prostate development and cancer. Genes Dev 1999;13:966–77.
9. Kim MJ, Cardiff RD, Desai N, et al. Cooperativity of Nkx3.1 and Pten loss of function in a mouse model of prostate carcinogenesis. Proc Natl Acad Sci U S A 2002;99:2884–9.
10. Magee JA, Abdulkadir SA, Milbrandt J. Haploinsufficiency at the Nkx3.1 locus. A paradigm for stochastic, dosage-sensitive gene regulation during tumor initiation. Cancer Cell 2003;3:273–83.
11. Li QL, Ito K, Sakakura C, et al. Causal relationship between the loss of RUNX3 expression and gastric cancer. Cell 2002;109:113–24.
12. Cameron ER, Neil JC. The Runx genes: lineage-specific oncogenes and tumor suppressors. Oncogene 2004;23:4308–14.
13. Gidekel S, Pizov G, Bergman Y, Pikarsky E. Oct-3/4 is a dose-dependent oncogenic fate determinant. Cancer Cell 2003;4:361–70.
14. Korkmaz CG, Korkmaz KS, Manola J, et al. Analysis of androgen regulated homeobox gene NKX3.1 during prostate carcinogenesis. J Urol 2004; 172:1134–9.
15. Heiden T, Wang N, Tribukait B. An improved Hedley method for preparation of paraffin-embedded tissues for flow cytometric analysis of ploidy and S-phase. Cytometry 1991;12:614–21.
16. Zhang Y, Glass A, Bennett N, Oyama KA, Gehan E, Gelmann EP. Long-term outcomes after radical prostatectomy performed in a community-based health maintenance organization. Cancer 2004;100:300–7.
17. Zellweger T, Ninck C, Mirlacher M, et al. Tissue microarray analysis reveals prognostic significance of syndecan-1 expression in prostate cancer. Prostate 2003;55:20–9.
18. Nakayama T, Watanabe M, Suzuki H, et al. Epigenetic regulation of androgen receptor gene expression in human prostate cancers. Lab Invest 2000;80:1789–96.
19. He WW, Sciavolino PJ, Wing J, et al. A novel human prostate-specific, androgen-regulated homeobox gene (NKX3.1) that maps to 8p21, a region frequently deleted in prostate cancer. Genomics 1997;43:69–77.
20. Rao J, Seligson D, Hemstreet GP. Protein expression analysis using quantitative fluorescence image analysis on tissue microarray slides. Biotechniques 2002;32: 924–30, 932.
21. Esteller M, Sparks A, Toyota M, et al. Analysis of adenomatous polyposis coli promoter hypermethylation in human cancer. Cancer Res 2000;60:4366–71.
22. Xu LL, Srikantan V, Sesterhenn IA, et al. Expression profile of an androgen regulated prostate specific homeobox gene NKX3.1 in primary prostate cancer. J Urol 2000;163:972–9.
23. Kim MJ, Bhatia-Gaur R, Banach-Petrosky WA, et al. Nkx3.1 mutant mice recapitulate early stages of prostate carcinogenesis. Cancer Res 2002;62:2999–3004.
24. Steadman DJ, Giuffrida D, Gelmann EP. DNA-binding sequence of the human prostate-specific homeodomain protein NKX3.1. Nucleic Acids Res 2000;28:2389–95.
25. Carson JA, Fillmore RA, Schwartz RJ, Zimmer WE. The smooth muscle γ-actin gene promoter is a molecular target for the mouse bagpipe homologue, mNkx3-1, and serum response factor. J Biol Chem 2000;275:39061–72.
26. Gelmann EP, Steadman DJ, Ma J, et al. Occurrence of NKX3.1 C154T Polymorphism in men with and without prostate cancer and studies of its effect on protein function. Cancer Res 2002;62:2654–9.